

# Spin-Waves in the Mid-Infrared Spectrum of Antiferromagnetic $\text{YBa}_2\text{Cu}_3\text{O}_{6.0}$

M. Grüninger, J. Münzel, A. Gaymann, A. Zibold and H. P. Geserich  
*Institut für angewandte Physik, Universität Karlsruhe, D-76128 Karlsruhe, Germany*

T. Kopp  
*Institut für Theorie der kondensierten Materie, Universität Karlsruhe*  
(June 18, 2021)

The mid-infrared spin-wave spectrum of antiferromagnetic  $\text{YBa}_2\text{Cu}_3\text{O}_{6.0}$  was determined by infrared transmission and reflection measurements ( $\mathbf{k} \parallel \mathbf{c}$ ) at  $T = 10$  K. Excitation of single magnons of the optical branch was observed at  $E_{\text{op}} = 178.0$  meV. Two further peaks at 346 meV ( $\approx 1.94 E_{\text{op}}$ ) and 470 meV ( $\approx 2.6 E_{\text{op}}$ ) both belong to the two-magnon spectrum. Linear spin wave theory is in good agreement with the measured two-magnon spectrum, and allows to determine the exchange constant  $J$  to be about 120 meV, whereas the intrabilayer coupling  $J_{12}$  is approximately  $0.55 J$ .

74.72.-h, 74.25.Gz, 74.25.Ha, 78.30.-j, 75.30.Ds

High temperature superconductors are basically layered copper-oxide materials. It is widely accepted that the relevant electronic degrees of freedom are confined to copper-oxide planes. The number of  $\text{CuO}_2$  planes per unit cell varies: e.g.,  $\text{La}_{2-x}\text{Sr}_x\text{CuO}_4$  exists in a single plane form with a large spacing between planes of  $\approx 13.2 \text{ \AA}$ , and  $\text{YBa}_2\text{Cu}_3\text{O}_{6+x}$  has a double layer structure with intra- and interbilayer spacings of  $\approx 3.3 \text{ \AA}$  and  $8.5 \text{ \AA}$ , respectively. Electronic correlations, and hence spin dynamics [1], may depend on the type of stacking of the planes. More specifically, a sizable coupling  $J_{12}$  between spins on adjacent planes of a bilayer will influence the spin excitation spectrum as well as the nature of the ground state. This may have been seen already in doped compounds: the normal state spin susceptibility of  $\text{La}_{2-x}\text{Sr}_x\text{CuO}_4$  extrapolates to a finite value at zero temperature, whereas it extrapolates to zero for  $\text{YBa}_2\text{Cu}_3\text{O}_{6.6}$  [2]. This may be interpreted as a signature for the opening of a spin excitation gap in  $\text{YBa}_2\text{Cu}_3\text{O}_{6.6}$  at low temperatures [3]—a behavior certainly not encountered in Fermi liquids. Further, a spin density wave ordering for  $\text{La}_{2-x}\text{Sr}_x\text{CuO}_4$  has been proposed, but for  $\text{YBa}_2\text{Cu}_3\text{O}_{6.6}$  a singlet pairing of spins in adjacent  $\text{CuO}_2$  planes with strong antiferromagnetic fluctuations within a plane [4,2,5]. Such a scenario seems to require an unrealistically large  $J_{12} \gtrsim 2.5J$  [6], where  $J$  is the in-plane exchange coupling of the Heisenberg Hamiltonian supposed to describe the low energy spin dynamics of a single bilayer for zero doping ( $x = 0$ ). However it was argued that, for finite doping, the itinerant carriers destroy the antiferromagnetism of the insulating phase and, therefore, much smaller values of  $J_{12}$  will produce a singlet interplane pairing in the conducting phase of  $\text{YBa}_2\text{Cu}_3\text{O}_{6.6}$ .

Up to now, no experimental evidence has been given of a sizable bilayer coupling ( $J_{12} \sim J$ ). In neutron-scattering experiments on  $\text{YBa}_2\text{Cu}_3\text{O}_{6+x}$ , the in-plane coupling was determined from the dispersion of acoustic spin-waves and was found to be extremely large ( $J = 120 \pm 20$  meV [7],  $J = 150$  meV [8], both for  $x = 0.15$ ). Yet, no optical modes have been found for energies up to 60 meV [7,9], suggesting a bilayer coupling of  $J_{12} \gtrsim 8$  meV. In Raman-

scattering experiments on  $\text{YBa}_2\text{Cu}_3\text{O}_{6+x}$  a two-magnon peak was observed [10,11].  $J$  was found to be consistent with the neutron-scattering data, whereas  $J_{12}$  was neglected.

In this Letter we report the first observation of an optical magnon peak and of the two-magnon spectrum in infrared spectroscopy of  $\text{YBa}_2\text{Cu}_3\text{O}_{6.0}$ . They allow to determine both  $J_{12}$  and  $J$ . Two resonances of the two-magnon spectrum confirm the location of the single magnon peak. Further, understanding the ‘antiferromagnetic limit’  $\text{YBa}_2\text{Cu}_3\text{O}_{6.0}$  will be crucial to interpret the excitations of carriers in doped  $\text{YBa}_2\text{Cu}_3\text{O}_{6+x}$  [12].

Due to the high resolution and the wide spectral range, optical spectroscopy is a powerful method to determine precisely energies of spin-waves. But, compared to other optical excitations such as infrared-active phonons, intraband and interband transitions, the absorption by magnons is two to three orders of magnitude weaker, yielding an optical conductivity of the order of 1 S/cm. Therefore, spin-wave excitations can be detected only in the transmittance spectra of thin single crystals. Up to now, investigations of this type have only been performed on single layer cuprates [13]. Broad structures between 0.4 eV and 1.2 eV were observed which were interpreted as an exciton and magnon-sidebands [13].

The crystals with typical dimensions of  $1 \times 1 \times 0.1 \text{ mm}^3$  had been annealed in the UHV at 700 K for two days to exclude doping by excess oxygen. The samples are very close to the pure limit  $\text{YBa}_2\text{Cu}_3\text{O}_{6.0}$  showing values of the conductivity function lower than 0.1 S/cm which is about three (five) orders of magnitude smaller than in  $\text{YBa}_2\text{Cu}_3\text{O}_{6.1}$  ( $\text{YBa}_2\text{Cu}_3\text{O}_7$ ) in the same spectral range. The measurements were performed using a Fourier transform spectrometer Bruker IFS 113v in the spectral range between 85 meV and 1.5 eV. The samples were mounted on a diaphragm in a helium-flow cryostat. Reference spectra at each temperature were obtained using a second, identical diaphragm and a turning mechanism. Hence an absolute photometric accuracy of the transmission data of about 1% was achieved.

The conductivity function  $\sigma(\hbar\omega) = 2\omega\varepsilon_0 n(\hbar\omega)k(\hbar\omega)$  can be calculated, if the sample thickness and both transmission and reflection spectra are known. Here,  $n$  and  $k$  denote the real and imaginary part of the refractive index. The sample thickness could be determined precisely from the spectral position of the interference maxima. Since reflection and transmission measurements use slightly different incident angles, and as furthermore the incident light beams are not completely parallel, there are still small interference structures in our plot of  $\sigma(\hbar\omega)$ .

In the upper panels of Fig. 1 reflectance and transmittance spectra, obtained at  $T = 10 \text{ K}$  on a single-crystalline platelet with a thickness of  $d = 125 \mu\text{m}$ , are displayed. The resulting conductivity function is shown in the lower panel of the same figure. Between 0.1 eV and 0.4 eV the measurements are dominated by interference effects, indicating regions of low absorption (as can be seen in  $\sigma$ ). Whereas the interference structure was precisely resolved by the spectrometer it cannot be resolved in the figure.

The reflectance spectrum by itself is not sufficient to determine the excitations present in this spectral range, only the knowledge of both reflectance and transmittance provides full information. To discuss the different excitations a plot of  $\sigma(\hbar\omega)$  is most suitable. There, the exponentially decreasing high energy tail of the highest fundamental phonon mode is observed up to 0.15 eV. Several smaller structures due to absorption by multi-phonons are superimposed on it. The main absorption features in the mid-infrared region are of

magnonic origin. The excitation of single-magnons of the optical branch is observed at  $E_{\text{op}} = 178.0$  meV. The two peaks marked  $E_{2a}$  and  $E_{2b}$  both belong to the two-magnon spectrum, as will be discussed below. The broad high energy tail of the spectrum is caused by higher multi-magnons. Finally, the steep increase of conductivity above 1.3 eV is due to the onset of intrinsic absorption, the excitation of carriers across the charge transfer gap.

In order to interpret this magnon spectrum, we use linear spin wave theory (LSW) to gain the excitation spectrum of localized spins on a bilayered square lattice. A Heisenberg Hamiltonian accounts for these low energy excitations for zero doping:

$$H = J \sum_{a=1,2} \sum_{\langle i,j \rangle} \mathbf{S}_{a,i} \mathbf{S}_{a,j} + J_{12} \sum_i \mathbf{S}_{1,i} \mathbf{S}_{2,i} \quad (1)$$

where  $i$  and  $j$  label nearest neighbor sites in a two-dimensional square lattice and  $a \in \{1, 2\}$  labels the two different planes in a single bilayer. Each bond is counted once. Generally it is found that LSW supplies quantitatively satisfying results for the Néel ground state at low temperatures [14,15,1]. The (classical) Néel ground state  $\mathbf{S}_{1,2,i} = \pm(-1)^i S(1, 0, 0)$  is stabilized by a finite bilayer coupling  $J_{12}$  [16] ( $S = 1/2$ ). Spin-orbit effects are relatively small [16] and were neglected in Eq. (1). However, the finite spin-orbit coupling is needed to couple the external electric field to a single magnon, and further to make two-magnon absorption possible for the considered crystal symmetry [17].

Due to the finite bilayer coupling, the classical one-magnon spectrum splits into acoustic and optical branches [18]:

$$\hbar \omega_{\text{op/ac}}(\mathbf{k}) = SJ \sqrt{z^2 - \tau_{\mathbf{k}}^2 + 2(J_{12}/J) \cdot (z \pm \tau_{\mathbf{k}})} \quad (2)$$

where  $z=4$  is the coordination number in a plane, and  $\tau_{\mathbf{k}} = 2(\cos(k_x a) + \cos(k_y a))$ .  $\mathbf{k}$  is within the magnetic Brillouin zone, and  $a$  is the lattice constant. Absorption experiments probe  $\mathbf{k}=0$  with energy gap

$$E_{\text{op}} \equiv \hbar \omega_{\text{op}}(\mathbf{k}=0) = 2(2S)\sqrt{J_{12}J} \quad (3)$$

for the optical branch. The acoustic mode splits, due to the small spin-orbit coupling [16]. The gapped out-of-plane mode is indeed observed in neutron-scattering experiments at  $E_{\text{ac}}(\mathbf{k}=0) \approx 4.5$  meV [9]. The splitting of the optical branch at  $\mathbf{k}=0$  may be estimated to be  $\Delta E_{\text{op}} \approx E_{\text{ac}}^2/2E_{\text{op}} \approx 1/18$  meV, a scale too small in comparison to the width of the optical magnon peak of about 1 meV to be resolved in our experiment.

The two-magnon absorption is calculated with a coupling Hamiltonian of the form

$$H_1 = D \sum_{a,b} \sum_{\langle i,j \rangle} \mathbf{E} \cdot [(\mathbf{S}_{a,i} \times \mathbf{S}_{b,j}) \times \boldsymbol{\pi}_{a,i;b,j}] \quad (4)$$

where  $\boldsymbol{\pi}_{a,i;b,j}$  points in the direction of the vector joining the pair  $\langle a, i; b, j \rangle$  and  $\mathbf{E}$  is the electric field vector [19]. This is the only coupling allowed by crystal symmetry for a nearest neighbor two-magnon generation [20].  $D\boldsymbol{\pi}$  is found from a perturbation series in the long-wavelength electron-photon and spin-orbit interaction [17]. Since we restrict ourselves to

$\mathbf{k}||c$ , the two-magnon coupling is proportional to  $E^y \pi_{1,i;2,i}^z \cdot (S_{1,i}^- S_{2,i}^+ - S_{1,i}^+ S_{2,i}^-)$  which creates a singlet pair of magnons on adjacent planes.

Absorption is not just determined by the convoluted density of states (DOS) of two magnons but also by the (local) interaction between the two magnons [19]. Therefore, absorption is not just characterized by a step-like increase at the optical two-magnon edge,  $2E_{\text{op}}$ , and a diverging DOS at the upper band edge (as for  $J_{12} = 0$ ). Rather, the local interaction will reduce the frustration produced by the two spinflips and allow two optical magnons to form a nearly bound state below  $2E_{\text{op}}$ . Due to the admixture of acoustic magnons the bound state shows up as a resonance (see Fig. 2). A second broader resonance close to the band edge replaces the diverging two-magnon DOS for  $J_{12} > 0$ , similar to the well-known two-magnon peak in  $B_{1g}$  Raman scattering. Quantum fluctuations certainly broaden the two-magnon peaks.

The exact positions of both peaks depend upon the ratio  $J_{12}/J$ , as is displayed in the inset of Fig. 2. Comparison with experiment yields a value of  $0.55 \pm 0.05$  for this ratio (0.53 for  $E_{2a}$  and 0.58 for  $E_{2b}$ ). Hence both resonances confirm the interpretation of the peak at  $E_{\text{op}}$  as a single magnon process. The calculated minimum at  $2 \cdot E_{\text{op}} = 356.0 \text{ meV}$  is also present in our measurements (see inset of Fig. 1). With  $E_{\text{op}} = 178 \text{ meV}$  and Eq. (3) we obtain  $J \approx 120 \text{ meV}$  and  $J_{12} \approx 66 \text{ meV}$ . For comparison, the calculated absorption spectrum for  $J_{12}/J = 1$  is given by the dashed line in Fig. 2 which demonstrates that the shape has changed qualitatively, quite distinct from the measured spectrum. Actually, the resonance at  $E_{2b}$  is lost for  $J_{12}/J \gtrsim 0.6$  [21] and is replaced by a broad hump.

The amazingly high value of  $J_{12}$  implies that the bilayer coupling may not be neglected in the interpretation of any experiment with  $\text{YBa}_2\text{Cu}_3\text{O}_6$ . The slope of the magnon dispersion as measured in neutron scattering is  $\sqrt{2} 2S J \sqrt{1 + \frac{1}{4} J_{12}/J} \simeq \sqrt{2} (J + J_{12}/8)$ , but  $J_{12}/8$  is still a small correction within experimental uncertainty. Raman-scattering results should depend on  $J_{12}$  more visibly: The calculated zone boundary two-magnon peak in  $B_{1g}$  geometry is located at approximately  $E_{B_{1g}} \simeq 2.7J + J_{12}$  in LSW (Fig. 3). That is, the excitation is a nearly local two-magnon state in a single plane with energy  $(2Sz-1)J + 2S J_{12}$  (cf. [19]), and delocalization reduces the frustration in the plane. This calculated peak position differs from that of recent experiments [11] by about +15%. But, the standard Fleury-Loudon scattering Hamiltonian [22]  $H_{\text{FL}}$ , which describes the interaction of spin pairs with light through a spin-exchange process, has to be drastically corrected for the high incident energies [23]. These are always above the charge transfer gap. Though, we only expect a minor shift of the two-magnon peak position.

We propose that a major shift may result from coupling to phonons: It was shown that the unexpected large width  $\Delta E_{B_{1g}}$  of the Raman peak may be explained by such a coupling which is effective *only for zone boundary magnons* [24,25]. This mechanism may be responsible for a shift of the  $B_{1g}$  Raman peak of the order of  $(\Delta E_{B_{1g}}/E_{B_{1g}})^2$  but will effect the absorption peaks of Fig. 2 only little.

Moreover, in  $A_{1g}$  scattering geometry, which emphasizes the zone center, a broad resonance is observed at  $E_{A_{1g}} \approx 350 \text{ meV}$  [26]. We expect this zone center peak not to be shifted by phonons. Indeed, LSW reproduces such a broad feature with a maximum close to the measured  $E_{A_{1g}}$  (inset of Fig. 3). To ensure that  $A_{1g}$ -scattering vanishes for  $J_{12} = 0$ , fluctu-

ations of the longitudinal component  $S_i^x S_j^x$  have to be added to the response functions [19] (inset of Fig. 3, dashed line). Although a consistent calculation including these fluctuations is beyond LSW the trend of such a correction is clearly seen: the asymmetry of the  $A_{1g}$  resonance is more pronounced, and the intensity is reduced. However, even if the shape is reproduced correctly, other processes, such as next nearest neighbor contributions to  $H_{FL}$ , may be as important. Besides, also single layered cuprates exhibit a  $A_{1g}$  resonance which does not result from  $H_{FL}$ .

In conclusion, we presented the low conductivity mid-infrared spectrum of  $\text{YBa}_2\text{Cu}_3\text{O}_{6.0}$ , which is dominated by absorption due to magnons. By comparison with linear spin wave theory we could determine the ratio  $J_{12}/J = 0.55 \pm 0.05$  and hence  $J \approx 120$  meV and  $J_{12} \approx 66$  meV.

We are indebted to P. Wölfle for many helpful discussions and his encouragement, and we also acknowledge useful discussions with A. Rosch. This work was supported by the Commission of the EC under contract no. CI 1-0526-M(CD) and by the High- $T_c$  program of Baden-Württemberg. It was supported in part by the DFG (M.G., H.P.G.) and by SFB 195 (T.K.).

- 
- [1] recent reviews on this topic are: A.P. Kampf, Phys. Rep. **249**, 219 (1994), and W. Brenig, Phys. Rep. (first months 1995).
  - [2] A.J. Millis, H. Monien, Phys. Rev. Lett. **70**, 2810 (1993); Phys. Rev. Lett. **71**, 210(E) (1993).
  - [3] other underdoped double and triple layer cuprates display a similar behavior; for references see [1].
  - [4] B.L. Altshuler, L.B. Ioffe, Solid State Commun. **82**, 253 (1992).
  - [5] M.U. Ubbens, P.A. Lee, Phys. Rev. B **50**, 438 (1994).
  - [6] A.W. Sandvik, D.J. Scalapino, Phys. Rev. Lett. **72**, 2777 (1994).
  - [7] S. Shamoto, M. Sato, J.M. Tranquada, B.J. Sternlieb, G. Shirane, Phys. Rev. B **48**, 13817 (1993).
  - [8] J. Rossat-Mignod, L.P. Regnault, J.M. Jorgensen, P. Burlet, J.Y. Henry, G. Lapertot, in *Dynamics of Magnetic Fluctuations in High-Temperature Superconductors*, ed. by G. Reiter, P. Horsch and G.C. Psaltakis (Plenum Press, New York, 1989).
  - [9] C. Vettier, P. Burlet, J.Y. Henry, M.J. Jurgens, G. Lapertot, L.P. Regnault, J. Rossat-Mignod, Phys. Scripta T29, 110 (1989).
  - [10] K.B. Lyons, P.A. Fleury, L.F. Schneemeyer, J.V. Waszczak, Phys. Rev. Lett. **60**, 732 (1988).
  - [11] S. Sugai et al., Phys. Rev. B **42**, 1045 (1990).
  - [12] M. Grüninger, A. Zibold, J. Münzel, A. Gaymann, H.P. Geserich, T. Kopp, to be published.
  - [13] J.D. Perkins, J.M. Graybeal, M.A. Kastner, R.J. Birgeneau, J.P. Falck, M. Greven, Phys. Rev. Lett. **71**, 1621 (1993).
  - [14] S. Chakravarty, B.I. Halperin, D.R. Nelson, Phys. Rev. B **39**, 2344 (1989).
  - [15] E. Manousakis, Rev. Mod. Phys. **63**, 1 (1991).
  - [16] N.E. Bonesteel, Phys. Rev. B **47**, 11302 (1993).
  - [17] N.E. Moriya, J. Appl. Phys. **39**, 1042 (1968), and references therein.

- [18]  $J_{12} = 2J_{12,\text{Bonesteel}}$  of ref.[15], eqs. (5.16) ff.
- [19] R.J. Elliott, M.F. Thorpe, J. Phys. C **2**, 1630 (1969).
- [20] Actually, due to the buckling of the in-plane  $\text{O}^{2-}$  ions towards the  $\text{Y}^{3+}$  ions, the center of inversion located at the midpoint between 2 nearest neighbor in-plane spins is lost. Therefore, a contribution from  $\mathbf{S}_{a,i} \cdot \mathbf{S}_{a,j}$  is allowed though small at  $J_{12}/J = 0.55$  (dashed line in Fig. 3, inset). It will broaden the absorption peaks but shift their position only by a negligible amount.
- [21] i.e., the real part of the denominator of the response function has no zero at  $E_{2b}$  for  $J_{12}/J \gtrsim 0.6$ .
- [22] P.A. Fleury, R. Loudon, Phys. Rev. **166**, 514 (1968).
- [23] A.V. Chubukov, D.M. Frenkel, to be published.
- [24] P. Knoll, C. Thomsen, M. Cardona, P. Murugaraj, Phys. Rev. B **42**, 4842 (1990).
- [25] D.U. Sanger, Phys. Rev. B **49**, 12176 (1994).
- [26] K.B. Lyons, P.A. Fleury, R.R.P. Singh, P. Sulewski, in the book of reference [9], p.159.

FIG. 1. Upper panels: In-plane reflectance and transmittance spectra ( $\mathbf{k}||c$ ) of a  $\text{YBa}_2\text{Cu}_3\text{O}_{6.0}$  single crystal with  $d=125\mu\text{m}$  at  $T=10\text{ K}$ . The arrows mark absorption processes described in the text. Lower panel: The resulting optical conductivity function.

FIG. 2. Calculated two-magnon absorption for  $J_{12}/J = 0.55$  (solid line) and 1.0 (dashed line) with  $\mathbf{k}||c$ ,  $T=0$ . Inset: Peak positions of the lower ( $E_{2a}$ ) and upper ( $E_{2b}$ ) two-magnon resonance in units of  $E_{\text{op}}$ . Arrows indicate the experimental values.

FIG. 3. Calculated Raman scattering in  $B_{1g}$  geometry for  $J_{12}/J=0.55$ ,  $T=0$ . The Raman shift  $\hbar\Delta\omega$  is displayed in units of  $E_{\text{op}}$  to compare the peak position to the position of the absorption resonances in Fig. 2. Inset:  $A_{1g}$  geometry in LSW (solid line), with corrections from longitudinal spin fluctuations (dashed line, scaled by a factor 3.5), both for  $J_{12}/J=0.55$ .

Fig. 2

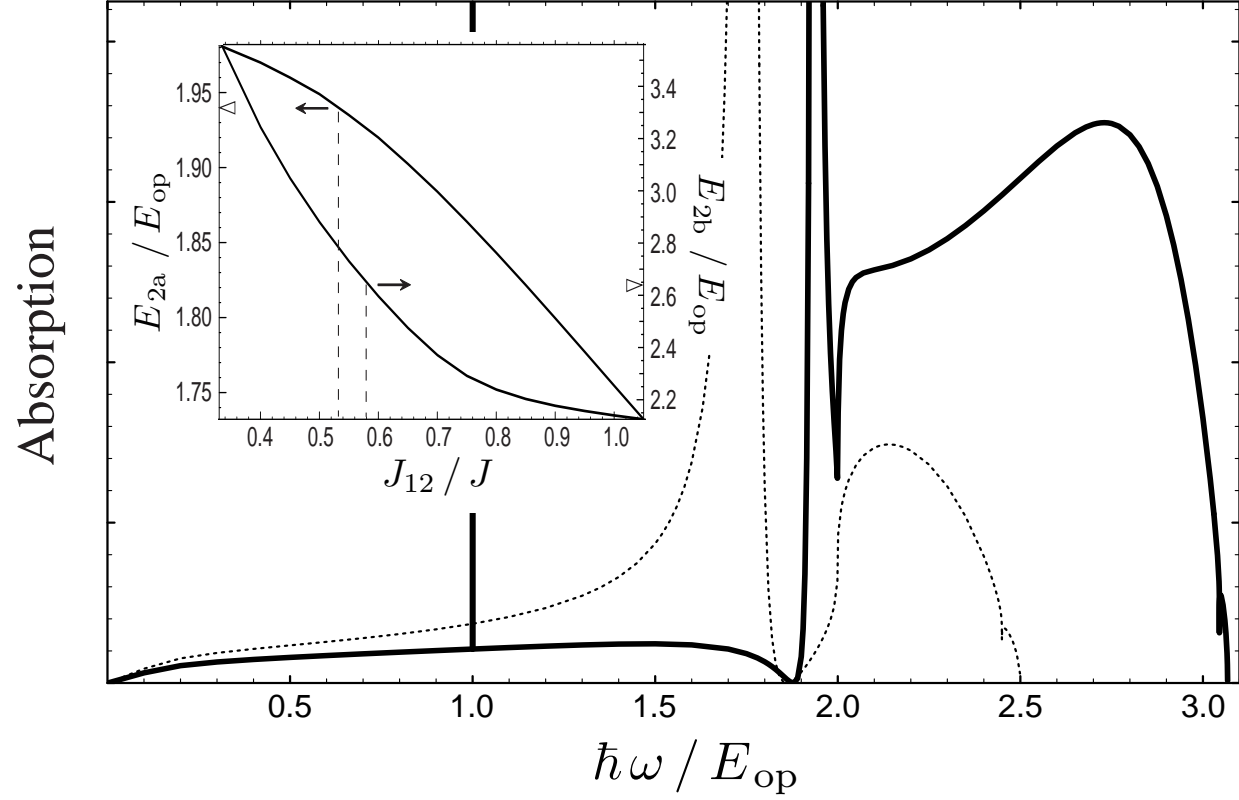


Fig. 1

